Thermochimica Acta, 224 (1993) 183–191
Elsevier Science Publishers B.V., Amsterdam

Kinetic studies of $LaNi_5$ hydride formation in non-isothermal conditions

C. Bayane [a,*], E. Sciora [b], N. Gerard [b] and M. Bouchdoug [a]

[a] *Laboratoire de Chimie-Physique, Département de Chimie, Faculté des sciences, Semlalia Université Cadi Ayyad, BP S 15, 40.000, Marrakech (Morocco)*
[b] *Laboratoire de Réactivité des Solides, Université de Dijon, BP 138, 21004 Dijon Cédex (France)*

(Received 18 January 1993; accepted 17 February 1993)

Abstract

Modelling studies are of practical importance in understanding and characterizing the kinetic behaviour of $LaNi_5$ hydride. Theoretical predictions describing the reaction kinetics under non-isothermal conditions are in good agreement with the experimental data obtained in our experiments.

INTRODUCTION

Numerous studies have been made in recent years on the hydriding reaction kinetics of $LaNi_5$ [1–13]. This material is currently of great interest because it exhibits a high hydrogen absorption capacity and good kinetic properties

$$LaNi_5 + 3H_2 \rightarrow LaNi_5H_6 \qquad \Delta H = -7 \text{ kcal per mol } H_2 \qquad (1)$$

The equilibrium pressure value is 2.5 atm at 25°C. Much attention has been devoted to developing models which explain the rapid reaction kinetics and reveal the rate-controlling process. It was believed that both intrinsic and non-intrinsic kinetic processes may control the rate, including diffusion, first-order processes, nucleation and growth, phase transformation, surface processes, heat and mass flow, etc.

Goodel and Rudman [8] compared $LaNi_5/H_2$ kinetics data from a number of laboratories and found that the results vary by as much as three orders of magnitude or more. This is due to a number of factors. For

* Corresponding author.

example, during successive hydriding and dehydriding cycles, the surface area and particle size continually change due to cracking [10]. We have already noted in a recent work that in the $LaNi_5/H_2$ system, fast exothermic reactions exhibit a complex relationship between the reaction rate and the sample mass [9]. In the early studies, isothermal and isobaric conditions were not maintained. Hence, mechanistic models for which isothermal conditions are assumed may often be inappropriate, although these are widely used.

Indeed, the reaction induces a heat accumulation which creates a temperature increase in the sample. Discrepancies can be expected due to different sample geometries and reactor designs among the various laboratories. Thus, the theoretical models that have usually been used to interpret the reaction kinetics in non-isothermal conditions, have often neglected the effect of the reactor (shape, material) and have considered only the effect of the sample bed.

EXPERIMENTAL PROCEDURE

Mass measurements were carried out in a high-pressure (0–1 MPa) microbalance with a limiting accuracy of 1 μg. The device was constructed from a genuine Setaram MTB 10-8 symmetrical beam-zero balance. In order to determine the sample temperature variation during the experiments, two thermocouples (A.T.E./B.T.E.) were positioned in the $LaNi_5$ and inert powder beds; the temperature gradient was evaluated as the temperature difference between these two samples. The sample holder was a cylindrical flat-bottomed cup, 0.5 mm thick, 5 mm deep and 10 mm in diameter. Another holder has the particular design shown in Fig. 1(b), consisting of a large lateral surface which ensures a maximum heat exchange with the surrounding gas phase.

These holders were machined from materials such as stainless steel, plexiglass and copper. The $LaNi_5$ compounds, prepared by induction melting of the pure components in a vacuum, were activated by performing about twenty absorption–desorption cycles ($T = 310$ K, $P_{H_2} = 1.5$ MPa) in order to pulverize the $LaNi_5$ samples into a homogeneous grain size (in the range 10–15 μm).

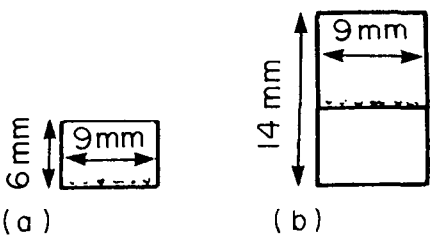

Fig. 1. Holder schemes: (a) small holder; (b) holder with large lateral surface.

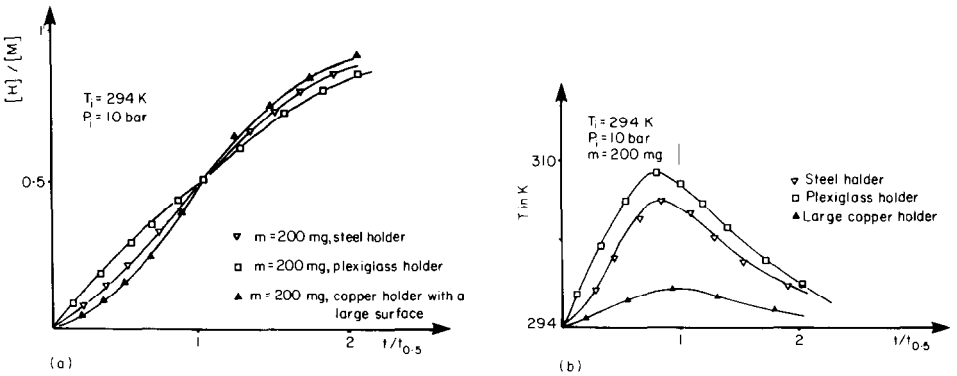

Fig. 2. (a) Formation curves: hydrogen fixed vs. time obtained with different holders; (b) temperature increase vs. time obtained with different holders.

EXPERIMENTAL RESULTS

The effect of the holder (material and shape)

The sample (about 200 mg) was scattered in the holder. Hydride formation with an activated sample was carried out at 294 K and 1 MPa, using different sample holders. The sample temperature variation as a function of reduced time $t/t_{0.5}$, where $t_{0.5}$ is the time required to have a reaction extent of [H]/[M] = 0.5, is reported in Fig. 2(b). The curves show a maximum that depends on the material of the holder. The temperature increase is important with holders of the form shown in Fig. 1(a). In the case of the copper holder, the sample temperature variation is comparable to the results obtained with the steel holder. In the case of the copper holder machined according to Fig. 1(b), the gas/holder interface is increased and temperature variation is halved. This difference also has an effect on the shape of the curve shown in Fig. 2(a), where the $LaNi_5$ hydrogen concentration [H]/[M] is reported versus reduced time $t/t_{0.5}$. The instantaneous maximum rate can be observed, either when first hydriding (in the case of the plexiglass holder), or during the course of hydriding (steel or copper holder). The maximum temperature increase coincides with the maximum slope (Fig. 2(a)) in the case of the large copper holder, as we have already noted [9].

Modification of the heat produced by increasing the mass

Hydride formations were carried out on $LaNi_5$ samples of different mass (10, 100, 200, 300 mg) under the same experimental conditions (T = 294 K,

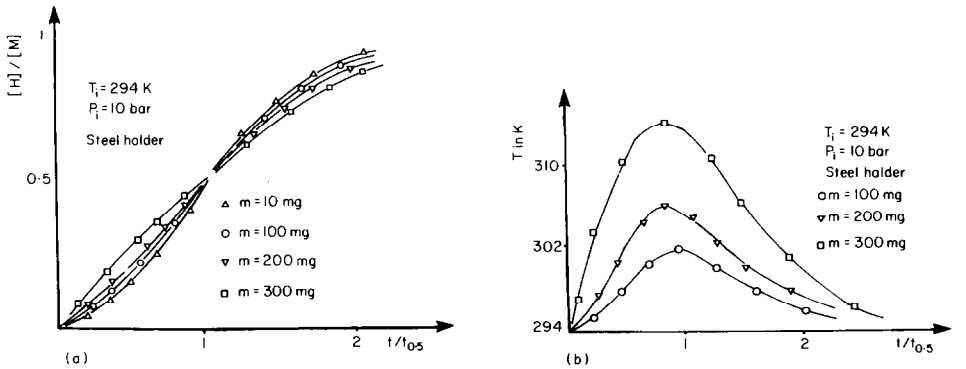

Fig. 3. (a) Formation curves: hydrogen fixed vs. time obtained with different sample masses; (b) temperature increase vs. time obtained with different sample masses.

$P = 1$ MPa). Figure 3 shows two families of curves, both functions of the reduced time $t/t_{0.5}$. It can be deduced that the sample temperature variation is greater when the sample mass is higher, and a decrease in the sample mass is manifested on the formation curves by a shorter nucleation period.

Analysis of transformation curves

Kinetic analysis of the data involves development of an analytical model representing the process over the broadest possible range of pressure, temperature and reaction extent.

The relation between reaction fraction α, pressure P, temperature T and time t, is represented as

$$f(\alpha) = Af(P)f(T)t \tag{2}$$

According to Delmon [14], the introduction of the reduced time $(t/t_{0.5})$ facilitates the comparison between experimental data and an advanced hypothetical model. Thus, for isothermal and isobaric test conditions, the reaction function $f(\alpha)$ is identifiable with specific reaction types, such as first-order reaction, diffusion, etc.

Next, optimal conditions for approaching an isothermal state are investigated and the development of the kinetic model is presented. The temperature and pressure functions are determined at fixed reaction extent and, finally, the reaction extent dependence is considered.

Isothermal conditions

In order to approach isothermal conditions, suitable the sample masses and holder materials have to be chosen.

Sample mass

For sample masses below 30 mg, the reactions are very fast. For example, for $m = 10$ mg the reaction time is less than one minute. However, the reaction time is about 10 min for a sample mass of 200 mg, but the sample temperature is generally higher than the imposed temperature.

We have selected a sample mass of 60 mg, which is a compromise between the two constraints.

Sample holder

The sample holder must have high great thermal conductivity and a large lateral surface to ensure a maximum heat exchange with the surrounding gas phase.

We have selected the copper holder with the large lateral surface.

When the experimental results are analysed, it can be concluded that

(i) The instantaneous rate expression is of the form

$$d\alpha/dt = A(P_i - P_e)\exp(-E_a/RT) \tag{3}$$

where A is a constant depending on sample activation, P_e is the thermodynamic equilibrium pressure, which can be expressed with thermodynamic parameters by $P_e = \exp(\Delta H - T\Delta S/RT)$, where P_i is the imposed pressure and E_a the activation energy value (23.5 kJ mol^{-1}).

(ii) The experimental reaction curves correspond with a nucleation-growth process which follows the Johnson and Mehl [15] equation

$$f(\alpha) = -\ln(1 - \alpha) = Kt^2 \tag{4}$$

The impact of perturbation, due to an insufficiency in the exchange of heat, on the evolution of the chemical act will now be considered.

Non-isothermal conditions

The heating of the test sample, which leads to deviation from isothermicity, is dependent on the reaction rate and thermal characteristics of the system. The produced heat is transferred from the sample to the holder and surrounding gas phase. The system temperature can be determined by the heat flow equation

$$(d\alpha/dt)\Delta n(\Delta H/2) + h(T(t) - T_i) = \sum m_i C_{pi} \frac{dT}{dt} \tag{5}$$

where $d\alpha/dt$ is the reaction rate, Δn is the sample size, ΔH is the reaction heat per mole of hydrogen, $\sum m_i C_{pi}$ is the heat capacity of the system

TABLE 1

Thermal transfer factors for the steel holder

T/K	m/mg	P/bar	h/(J s^{-1} K^{-1})
294	100	6	8.8×10^{-3}
294	100	7	8.5×10^{-3}
294	100	11	9.0×10^{-3}
294	200	5.2	9.2×10^{-3}
294	200	7.4	9.2×10^{-3}
294	200	9.5	9.0×10^{-3}
294	300	6	8.8×10^{-3}
294	300	8	9.5×10^{-3}
294	300	11	8.6×10^{-3}

(sample and holder), h is the thermal transfer factor which is dependent on the conductivities of the hydrogen sample and the holder material, the interface area between the holder and the surrounding gas, and the gas layer thickness, T_i is the laboratory tube temperature, and $T(t)$ is the actual sample temperature which depends on time. It was estimated that the measured temperature corresponds to an instantaneous mean effective operating temperature.

The inflexion point of the curves $[H]/[M] = f(t)$ corresponds to the highest temperature of the sample T_m. At this point, $(dT/dt) = 0$ and eqn. (5) can be written

$$(\Delta H/2)\Delta n(d\alpha/dt) + h(T(t) - T_i) = 0 \tag{6}$$

Thus, the factor h can be expressed as

$$h = -\frac{T_m - T_i}{d\alpha/dt} \times \frac{1}{\Delta n(\Delta H/2)} \tag{7}$$

From this equation, it follows that h must be constant for experiments carried out at different pressures, the sample being located in the same holder (Tables 1–3).

TABLE 2

Heat transfer factors for the plexiglass holder

T/K	m/mg	h/(J s^{-1} K^{-1})
294	200	5.3×10^{-3}
304	200	5.08×10^{-3}

TABLE 3

Heat transfer factors for the copper holder with large lateral surface

T/K	m/mg	h/(J s^{-1} K^{-1})
294	200	5.5×10^{-2}
304	200	5.3×10^{-2}
312	200	5.8×10^{-2}
322	200	4.8×10^{-2}

A comparison of the h values for different holder materials yields the conclusion that this thermal factor is dependent on the material conductivity and the holder dimensions.

Model applicable to variable temperature and pressure reaction conditions

The expression of the sample temperature change (eqn. (5)) was combined with the rate equation (eqn. (3)) to describe the reaction rate under non-isothermal conditions.

This facilitates direct comparison of the kinetic model with experimental results. Thus we can analyse the reaction extent function

$$d\alpha/dt = A2t(1-\alpha)(P_i - P_c)\exp(-E_a/RT)$$

$$(d\alpha/dt)\Delta n(\Delta H/2) + h(T(t) - T_i) = \sum m_i C_{pi}\, dT/dt$$

Converging simultaneous solutions of these two equations can be determined by iterative calculation. This permits calculation of the reaction extent, the corresponding instantaneous sample temperature and the reaction rate.

The use of this treatment to describe non-isothermal reaction behaviour is illustrated in Fig. 4, for different sample masses. Experimental and theoretical reaction curves are presented in Fig. 4(a) using the hydrogen concentration [H]/[M] = α versus reduced time ($t/t_{0.5}$) format, for the steel holder.

The use of the same sample holder corresponds to the use of the same value for the heat transfer coefficient h in the calculated curves. The isothermal function is included for comparison. It is interesting to note the shape change which occurs as the sample mass increases. In addition, for sample masses in the range 10–200 mg, the experimental and calculated results are in good agreement. The same remarks can be made for sample temperature variation versus reduced time. In contrast, for a sample mass of 300 mg which is characterized by a high heat accumulation, the experimental data deviate slightly from the calculated results.

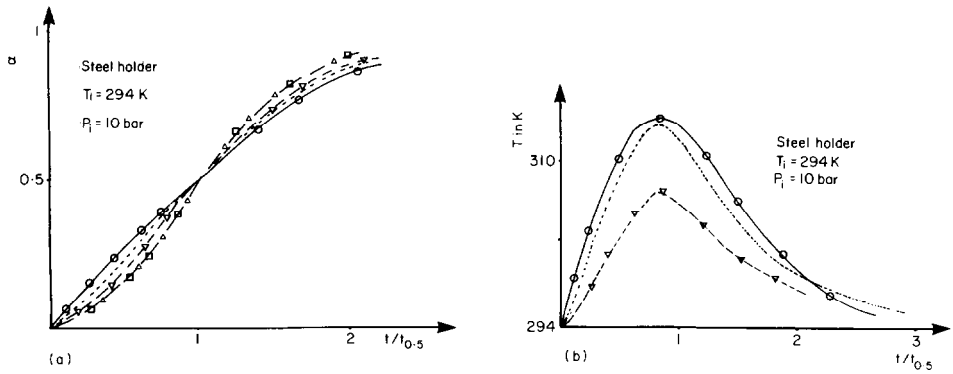

Fig. 4. (a) Formation curves: hydrogen concentration vs. time: △, isothermal curve ($m < 30$ mg, $h = 9 \times 10^{-3}$ J s^{-1} K^{-1}); experimental curves: (10 mg, □); (200 mg, ▽); (300 mg, ○). Calculated curves: – –, $m = 10$ mg, $h = 9 \times 10^{-3}$ J s^{-1} K^{-1}, $C = 0.27$ J K^{-1}; — — —, $m = 200$ mg, $h = 9 \times 10^{-3}$ J s^{-1} K^{-1}, $C = 0.36$ J K^{-1}; – – –, $m = 300$ mg, $h = 9 \times 10^{-3}$ J s^{-1} K^{-1}, $C = 0.40$ J K^{-1}; (b) temperature increase vs. time. Experimental curves: (200 mg, ▽); (300 mg, ○); calculated curves: ——, $m = 200$ mg, $h = 9 \times 10^{-3}$ J s^{-1} K^{-1}, $C = 0.36$ J K^{-1}; – – –, $m = 300$ mg, $h = 9 \times 10^{-3}$ J s^{-1} K^{-1}, $C = 0.40$ J K^{-1}.

The experimental and theoretical results obtained from studies performed using different sample holders are reported in Fig. 5. In the case of the sample holders machined from copper and steel, characterized by high thermal coefficients h and C, the experimental and calculated results are in good agreement. In the case of the plexiglass holder, characterized by low

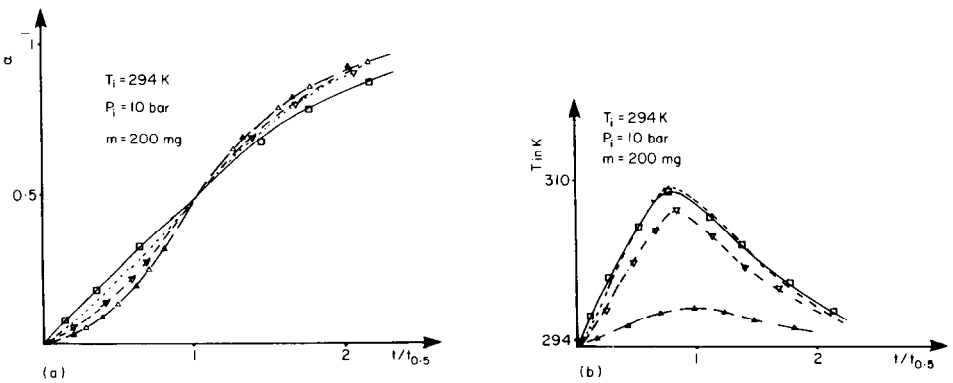

Fig. 5. (a) Formation curves: hydrogen concentration vs. time: △, isothermal curve ($h > 5 \times 10^{-2}$ J s^{-1} K^{-1}, $C > 1.4$ J s^{-1} K^{-1}); experimental curves: (copper, ▲); (steel, ▽); (plexiglass, □). Calculated curves: – –, $h = 5.3 \times 10^{-3}$ J s^{-1} K^{-1}, $C = 1.4$ J s^{-1} K^{-1} (copper holder); — — —, $h = 9 \times 10^{-3}$ J s^{-1} K^{-1}, $C = 0.35$ J K^{-1} (steel holder); – – –, $h = 5.2 \times 10^{-3}$ J s^{-1} K^{-1}, $C = 0.25$ J K^{-1} (plexiglass holder); (b) temperature increase vs. time. Experimental curves: (copper, ▲); (steel, ▽); (plexiglass, □); calculated curves: – –, $h = 5.3 \times 10^{-2}$ J s^{-1} K^{-1}, $C = 1.4$ J K^{-1} (copper holder); – – –, $h = 9 \times 10^{-3}$ J s^{-1} K^{-1}, $C = 0.35$ J K^{-1} (steel holder); - - -, $h = 5.2 \times 10^{-3}$ J s^{-1} K^{-1}, $C = 0.25$ J K^{-1} (plexiglass holder).

thermal coefficients h and C, we remark that the experimental data deviate slightly from calculated results.

DISCUSSION

In spite of the approximation adopted in the elaboration of this theoretical model, we have established the effects of the geometrical and thermal characteristics of the holder on the reaction kinetics. Thus, we have shown that the heat accumulation phenomenon can be manifested in the early stages of the reaction. This can affect, on one hand, the instantaneous rate and, on the other, the curve shape for the extent of reaction. In fact, in the case of great heat accumulation, the reaction can be fitted to a phase transformation or a first-order process. In contrast, in nearly isothermal conditions, the reaction kinetics corresponds to a nucleation and growth process. Therefore, the phase transformation or first-order process is a superficial consequence of the non-isothermal response.

REFERENCES

1 O. Boser, J. Less-Common Met., 46 (1976) 91.
2 S. Tanaka, J.D. Clewly and T.B. Flanagan, J. Phys. Chem., 81 (1977) 1684.
3 W.E. Wallace, R.F. Karlicek and H. Imamura, J. Phys. Chem., 83 (1979) 1708.
4 L. Schlapbach, J. Phys. F, 10 (1980) 2477.
5 G.D. Sandrock and P.D. Goodel, J. Less-Common Met., 73 (1980) 161.
6 N.C. Park and J.J. Lee, J. Less-Common Met., 83 (1982) 39.
7 P.S. Rudman, J. Less-Common Met., 89 (1983) 93.
8 P.D. Goodel and P.S. Rudman, J. Less-Common Met., 89 (1983) 117.
9 C. Bayane, M. EL Hammioui, E. Sciora and N. Gerard, J. Less-Common Met., 107 (1985) 213.
10 H. Uchida, K. Terao and Y.C. Huang, Z. Phys. Chem. N.F, 164 (1989) 1275.
11 D. Wen and S.J. Den, J. Less-Common Met., 155 (1989) 271.
12 J.T. Koh, A.J. Goody, P. Huang and G. Zhou, J. Less-Common Met., 153 (1989) 89.
13 U. Mayer, M. Groll and W. Supper, J. Less-Common Met., 131 (1989) 235.
14 B. Delmon, Introduction to Heterogeneous Kinetics, Technip Ed., Paris, 1969.
15 W.A. Johnson and F.F. Mehl, Trans. Am. Inst. Min. Metall. Pet. Eng., 135 (1939) 416.